THE EFFECT OF ASPECT AND CURVATURE RATIOS ON DOUBLE-DIFFUSIVE NATURAL CONVECTION IN A VERTICAL ANNULUS

M. A. Teamah
Mechanical Power Engineering Department,
Alexandria University, Alexandria, Egypt.

M. Shoukri
Mech. Eng. Dept. McMaster University,
Hamilton, Ontario, L8S 4L7, Canada.

ABSTRACT

A numerical study of double-diffusive natural convection in a vertical annular cavity is performed. The considered cavity is formed by two isothermal and iso-concentration concentric vertical cylinders, while the top and the bottom surfaces are considered adiabatic and impermeable. The flow, thermal and concentration fields within the annulus are examined for curvature ratios of $1 \leq K \leq 5$ and aspect ratios of $1 \leq Ar \leq 4$. The effect of the aspect and curvature ratios of the annulus on the average and local Nusselt and Sherwood numbers are studied in both aiding and opposing flow over the range of buoyancy ratio of $-10^3 \leq n \leq 10^3$. Finally the average Nusselt and Sherwood numbers are correlated in terms of buoyancy, aspect and curvature ratios. Throughout the calculations the Prandtl, Lewis, and solutal Rayleigh numbers are kept constant at 8.0, 10.0, and 10^5 respectively .

Keywords: Heat and mass transfer, Double, Diffusive, Natural, Convection.

NOMENCLATURE

Ar	Aspect ratio, H/R
C	Mass fraction
C^*	Dimensionless concentration, $[(C-C_o)/(C_i-C_o)]$
D	Mass diffusivity, m^2/s
g	Gravitational acceleration, m/s^2
Gr_m	Mass species Grashof number, $g\beta_m \Delta C R^3/\nu^2$
Gr_T	Thermal Grashof number, $g\beta_T \Delta T R^3/\nu^2$
h	Convective heat transfer coefficient, $W/m^2 K$
h_m	Convective mass transfer coefficient, m/s
k	Thermal conductivity, W/m K
K	Curvature ratio, r_o/r_i
H	Cavity height, m
Le	Lewis number, α/D
n	Buoyancy ratio, Gr_m/Gr_T
Nu	Average Nusselt number, h R/k
P	Pressure, Pa
P^*	Dimensionless pressure, $PR^2/\rho_r \alpha^2$
Pr	Prandtl number, ν/α
r	Radial coordinate, m
r^*	Dimensionless radial coordinates, r/R
R	Gap width, r_o-r_i
Ra_m	Mass species Rayleigh number, $g\beta_m \Delta C R^3/D\nu$
Ra_T	Thermal Rayleigh number, $g\beta_T \Delta T R^3/\alpha\nu$
Sc	Schmidt number, ν/D
Sh	Average Sherwood number, $h_m R/D$
T	Temperature, K
T^*	Dimensionless temperature, $[(T-T_o)/(T_i-T_o)]$
u	Radial velocity, m/s
u^*	Dimensionless radial velocity, uR/α
v	Axial velocity, m/s
v^*	Dimensionless axial velocity, vR/α
z	Axial coordinate, m
z^*	Dimensionless axial coordinate, z/R
α	Thermal diffusivity, m^2/s
β_m	Mass species expansion coefficient, m^3/Kg
β_T	Thermal expansion coefficient, 1/K
ν	Kinematic viscosity, m^2/s
ρ	Fluid density, Kg/m^3
ψ	Streamfunction

Subscripts

i	Inner wall
m	Mass species
o	Outer wall
r	Reference

T Thermal

Superscripts

* Dimensionless

1. INTRODUCTION

In the past, most researches have attended to the case of natural convection induced by temperature gradient as a single driving force. However, more recently attention has been paid to the simultaneous presence of two components with different diffusivities. This type of naturally convecting flow is referred to as double-diffusive natural convection. The double-diffusive flow has many engineering applications such as migration of contaminants, solar ponds, natural gas storage tanks, crystal growth technology, metal solidification process, drying process, heat exchanger fouling..etc. Also it has many physical applications such as the evaporation from the ocean and lake surfaces.

Early studies of the combined heat and mass transfer in enclosures were reported by Hu and EL-Wakil [1], Ostrach [2-4] and Lee et al. [5]. Recently Bejan et al. [6,7] conducted an analytical and numerical study of the combined heat and mass transfer in a vertical rectangular enclosure with uniform heat and mass fluxes along the vertical sides. They studied the effect of Lewis number by using a similarity solution. Viskanta et al. [8] examined the effect of combined lateral temperature and concentration gradients on natural convection in a two dimensional square cavity filled with a binary gas. The numerical study was limited to a simple additive flow where the Sc=Pr and the buoyancy ratio varied from -5 to 5. Numerical work on double-diffusive natural convection in a square cavity was more recently reported by Beghein et al. [9]. They correlated the heat and mass transfer rate in terms of Lewis, solutal Rayleigh and Schmidt numbers for heat or mass driven flows.

Han and Kuehn [10,11] studied experimentally and numerically the double-diffusive natural convection in a vertical rectangular enclosure. They presented a flow map showing the single and multi cell regions as a function of Lewis number and buoyancy ratio. The transient double-diffusive natural convection in a vertical rectangular enclosure was studied by Lee et al. [12,13]. They covered aiding and opposing flow due to horizontal temperature and concentration gradients for a rectangular cavity with aspect ratio of 2, solutal Rayleigh number of $6x10^7$ and buoyancy ratio in the range of 0.5 to 30. Lee [14] followed this transient study by studying the effect of boundary conditions on heat, mass transfer and flow structures in a rectangular enclosure with isothermal and impermeable vertical sides, while the top and the bottom were adiabatic and maintained at constant concentrations.

The combined heat and mass transfer in cylindrical geometries was recently examined by Shipp et al. [15-17]. They numerically investigated the steady laminar double-diffusive natural convection within a vertical annular cavity. An annulus with constant temperature and concentration differences imposed across the vertical walls was considered. Shipp [15] studied the effect of thermal Rayleigh number, buoyancy ratio, and Lewis number on the flow structure and average Nusselt and Sherwood numbers over the parametric ranges of $5x10^3 \leq Ra_T \leq 10^5$, $-10 \leq n \leq 10$, and $0.1 \leq Le \leq 10$, for an annulus having an aspect ratio of 1 and a curvature ratio of 2.

The present investigation extends the work of Shipp et al. [15-17] to cover the effect of aspect and curvature ratios on double-diffusive natural convection in a closed vertical annulus, when the cavity walls are at constant temperature and concentration. The effect of the annulus geometry on both the average and local Nusselt, and Sherwood numbers are studied. The study includes both cases of aiding and opposing buoyancy conditions, for a wide range of buoyancy ratio, $-1000 \leq n \leq 1000$. This range covers the entire range of mass diffusion dominated opposing and aiding flows as well as the thermal diffusion dominated flow. The aspect ratio of the considered annulus is varied from 1 to 4 and the radius ratio is varied from 1 to 5. The Prandtl, Lewis, and solutal Rayleigh numbers are set at 8,10 and 10^5 respectively. The wide range of buoyancy ratio covered in this work corresponds to varying the thermal Rayleigh number from -10^7 to 10^7 . The results are compared with published numerical and experimental results.

2. MATHEMATICAL FORMULATION

Figure (1) shows a schematic of the problem considered. An annulus with inner and outer radii of r_i and r_o respectively, and height H is formed by two co-axial vertical cylinders. The cylinders are isothermal and iso-concentration surfaces and the bottom and the top are adiabatic and impermeable surfaces. Qualitative description of the flow directions for both aiding and opposing buoyancy ratios were discussed by Han [11] and Shipp [15]. The flow in the cavity is considered to be steady and two dimensional. The fluid is assumed newtonian and nearly incompressible and the viscous dissipation is neglected. By introducing the above assumptions into the conservation equations of mass, momentum, energy, and mass species in cylindrical coordinates and using the Boussinsq approximation for the buoyancy term in the momentum equation, a set of governing equations is obtained as:

$$\frac{1}{r}\frac{\partial(r\,u)}{\partial r} + \frac{\partial v}{\partial z} = 0 \tag{1}$$

$$u\frac{\partial u}{\partial r} + v\frac{\partial u}{\partial z} = -\frac{1}{\rho_r}\frac{\partial P}{\partial r} + \nu\left[\frac{1}{r}\frac{\partial}{\partial r}\left[r\frac{\partial u}{\partial r}\right] - \frac{u}{r^2} + \frac{\partial^2 u}{\partial z^2}\right] \tag{2}$$

$$u\frac{\partial v}{\partial r} + v\frac{\partial v}{\partial z} = -\frac{1}{\rho_r}\frac{\partial P}{\partial z} + \nu\left[\frac{1}{r}\frac{\partial}{\partial r}\left[r\frac{\partial v}{\partial r}\right] - \frac{\partial^2 v}{\partial z^2}\right] + \frac{\rho_r - \rho}{\rho_r}g \tag{3}$$

$$u\frac{\partial T}{\partial r} + v\frac{\partial T}{\partial z} = \alpha\left[\frac{1}{r}\frac{\partial}{\partial r}\left[r\frac{\partial T}{\partial r}\right] - \frac{\partial^2 T}{\partial z^2}\right] \tag{4}$$

$$u\frac{\partial C}{\partial r} + v\frac{\partial C}{\partial z} = D\left[\frac{1}{r}\frac{\partial}{\partial r}\left[r\frac{\partial C}{\partial r}\right] - \frac{\partial^2 C}{\partial z^2}\right] \tag{5}$$

where

$$\rho = \rho_r\left[1 - \beta_m\left[T - T_r\right] - \beta_m\left[C - C_r\right]\right] \tag{6}$$

The above equations can be written in a dimensionless form by introducing the following dimensionless variables.

$$r^* = \frac{r}{R}\,,\quad u^* = \frac{u\,R}{\alpha}\,,\quad v^* = \frac{v\,R}{\alpha}\,,\quad P^* = \frac{P\,R^2}{\rho_r * \alpha^2}\,,\quad T^* = \frac{T - T_o}{T_i - T_o}\ \text{and}\ C^* = \frac{C - C_o}{C_i - C_o} \tag{7}$$

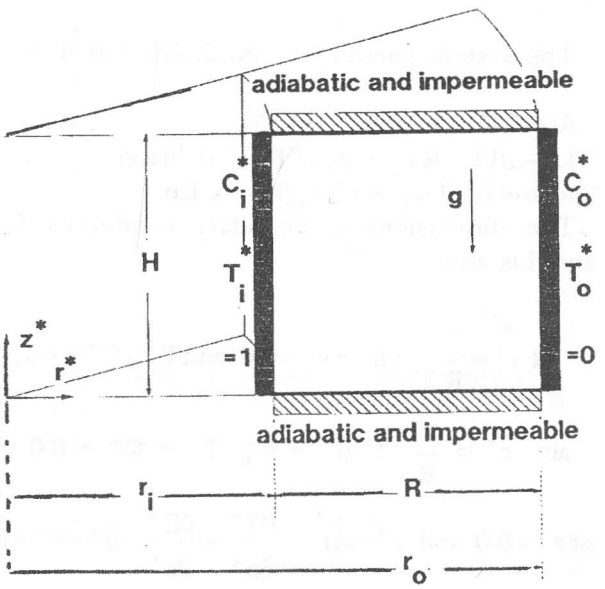

Figure 1. Schematic of enclosure.

Inserting the dimensionless variables, the governing equations will be as follows:

$$\frac{1}{r^*}\frac{\partial(r^*\,u^*)}{\partial r^*} + \frac{\partial v^*}{\partial z^*} = 0 \tag{8}$$

$$u^*\frac{\partial u^*}{\partial r^*} + v^*\frac{\partial u^*}{\partial z^*} = -\frac{\partial P^*}{\partial r^*} + Pr\left[\frac{1}{r^*}\frac{\partial}{\partial r^*}\left[r^*\frac{\partial u^*}{\partial r^*}\right] - \frac{u^*}{r^{*2}} + \frac{\partial^2 u^*}{\partial z^{*2}}\right] \tag{9}$$

$$u^*\frac{\partial v^*}{\partial r^*} + v^*\frac{\partial v^*}{\partial z^*} = -\frac{\partial P^*}{\partial z^*} + Pr\left[\frac{1}{r^*}\frac{\partial}{\partial r^*}\left[r*\frac{\partial v^*}{\partial r^*}\right] - \frac{\partial^2 v^*}{\partial z^{*2}}\right] + Ra_T\,Pr\left[T^* + nC*\right] \tag{10}$$

$$u^* \frac{\partial T^*}{\partial r^*} + v \frac{\partial T^*}{\partial z^*} = \left[\frac{1}{r^*} \frac{\partial}{\partial r^*} \left[r * \frac{\partial T^*}{\partial r^*} \right] - \frac{\partial^2 T^*}{\partial z^{*2}} \right] \quad (11)$$

$$u * \frac{\partial C^*}{\partial r^*} + v * \frac{\partial C^*}{\partial z^*} = \frac{1}{Le} \left[\frac{1}{r^*} \frac{\partial}{\partial r^*} \left[r * \frac{\partial C^*}{\partial r^*} \right] - \frac{\partial^2 C^*}{\partial z^{*2}} \right] \quad (12)$$

The system parameters are defined as flows:

$Ar=H/R$, $K=r_o/r_i$, $Pr=\nu/\alpha$,
$Le=\alpha/D$, $Ra_T = g\beta_T(T_i-T_o)R^3/(\nu\alpha)$
and $n=Gr_m/Gr_T = (Ra_m/R_T) \times Le$

The dimensionless boundary conditions for the annulus are:

$$\text{at } r^* = \frac{r_i}{R} \quad : u^* = v^* = 0.0 \text{ and } T^* = C^* = 1.0,$$

$$\text{at } r^* = \frac{r_o}{R} \quad : u^* = v^* = T^* = C^* = 0.0 , \quad (13)$$

$$\text{at } z^* = 0.0 \text{ and } z^* = Ar \; : \; \frac{\partial T^*}{\partial z^*} = \frac{\partial C^*}{\partial z^*} = u^* = v^* = 0.0$$

3. SOLUTION PROCEDURE

Finite difference equations are derived by integrating the governing differential equations over an elementary control volume. The coupling between the non-linear algebraic equations are handled using the SIMPLER algorithm discussed by Patankar [18]. The discretized equations obtained are solved iteratively line by line. Under-relaxation is required to ensure the convergence of the iterative procedure. The relaxation factor for the velocities was reduced to 0.03 for buoyancy ratio near unity, while in the other runs the best relaxation factor was 0.15.

A semi-uniform grid spacing is used in the axial direction. The size of five control volumes from both cavity ends are increased exponentially away to the cavity centre. In the radial direction a non-uniform grid spacing is used. The control volumes are fine adjacent to the cylinders and their width is increased exponentially to the power 1.5 away to the cavity centre. The number of grid points are dependent on the cavity aspect ratio: 35x35 for Ar=1.0, 35x65 for Ar=2.0, and 35x115 for Ar=4.

The solution is considered to be fully converged when the maximum value of the mass source and the change of the dependent variables are smaller than $5x10^{-5}$ per 50 iterations. The convergence was found to be very slow, specially at buoyancy ratios near unity. The number of iterations required to obtain a fully converged solution is approximately 1200 for single force-driven flows, and more than 5500 for double-diffusive dominated flows. During this investigation 144 runs were carried out.

The local Nusselt number, Nu_z on the inner cylinder is calculated as from,

$$Nu_z \quad \frac{h_z R}{k} = - \left[\frac{\partial T^*}{\partial r^*} \right]_{r^* = r_i^*} \quad (14)$$

The local Nusselt numbers are integrated to obtain the average Nusselt number Nu,

$$Nu = \frac{h R}{k} = \frac{1}{Ar} \int_0^{Ar} Nu_z \, dz^* \quad (15)$$

Similar equations are used to calculate the local and average Sherwood numbers. The local Sherwood number, Sh_z is given by:

$$Sh_z = \frac{h_{m_z} R}{D} = - \left[\frac{\partial C^*}{\partial r^*} \right]_{r^* = r_i^*} \quad (16)$$

and the average Sherwood number is given by:

$$Sh = \frac{h_m R}{D} = \frac{1}{Ar} \int_0^{Ar} Sh_z \, dz^* \quad (17)$$

4. RESULTS AND DISCUSSIONS

The code predictions were first validated against the results of De Vahl Davis [19,20] and El-Sherbiny and Teamah [21] for thermally induced natural convection in a closed annulus, with aspect ratio of $1 \le Ar \le 20$ and curvature ratio of $1 \le K \le 5$, in the range of thermal Rayleigh number of $10^3 \le Ra \le 10^6$. The predicted average Nusselt numbers were within 1% of those predicted by the others.

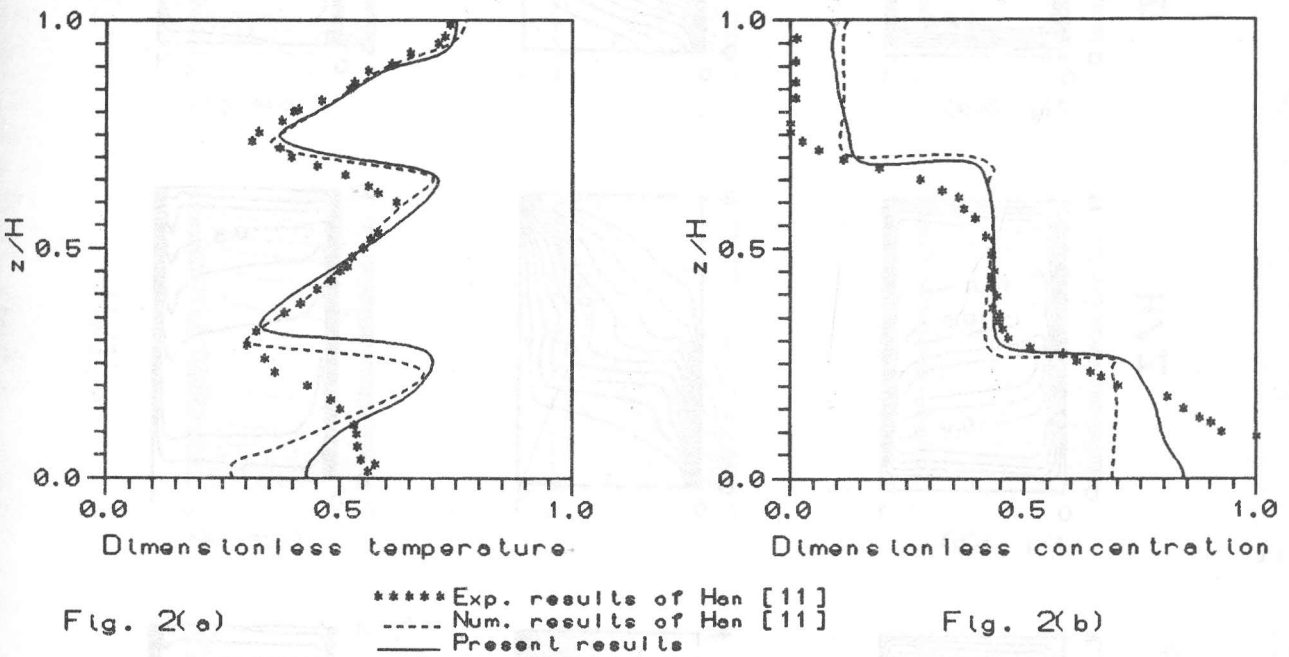

Figure 2. The temperature and concentration distribution along the vertical centre line in a rectangular cavity; Pr=8.0, Le=250.0, n=-7.5 and $Gr_T=6.25x10^3$; (a) Temperature and (b) Concentration.

The predictions of the present code were also validated against double-diffusive natural convection results obtained by Han [11] for a rectangular cavity having an aspect ratio of 4. Figure (2) shows the non-dimensional local temperature and concentration distribution along the centre line of the two-dimensional cavity for the case of Pr=8.0, Le=250, n=-7.5 and $Gr_T=6.25x10^3$ based on the cavity width, as predicted by the present code. The numerical predictions and the experimental results of Han [11] are also shown in Figure (2). As shown, the present results appear to be in better agreement with Han's experimental results than his numerical predictions, specially at the cavity ends. This is believed to be the result of using a semi-uniform grid in the vertical direction in the present investigation. Han [11] used a uniform grid in the vertical direction.

4.1. *Effect of Aspect Ratio on the Streamlines, Isotherms, and Concentration Isopleths.*

The annulus aspect ratio is varied from 1 to 4 with buoyancy ratio in the range of $-1000 \leq n \leq 1000$. The detailed results are shown herein for buoyancy ratios of 10 for aiding and -10 for opposing flows. The solutal Rayleigh number, Lewis number and annulus curvature ratio are set at 10^5, 10 and 2 respectively. The effect of aspect ratio on the flow field, and isopleths of temperature and concentration for the buoyancy ratio of 10, i.e. aiding flow, are shown in Figure (3). The left vertical boundary represents the inner cylinder with a constant dimensionless temperature and concentration of one,

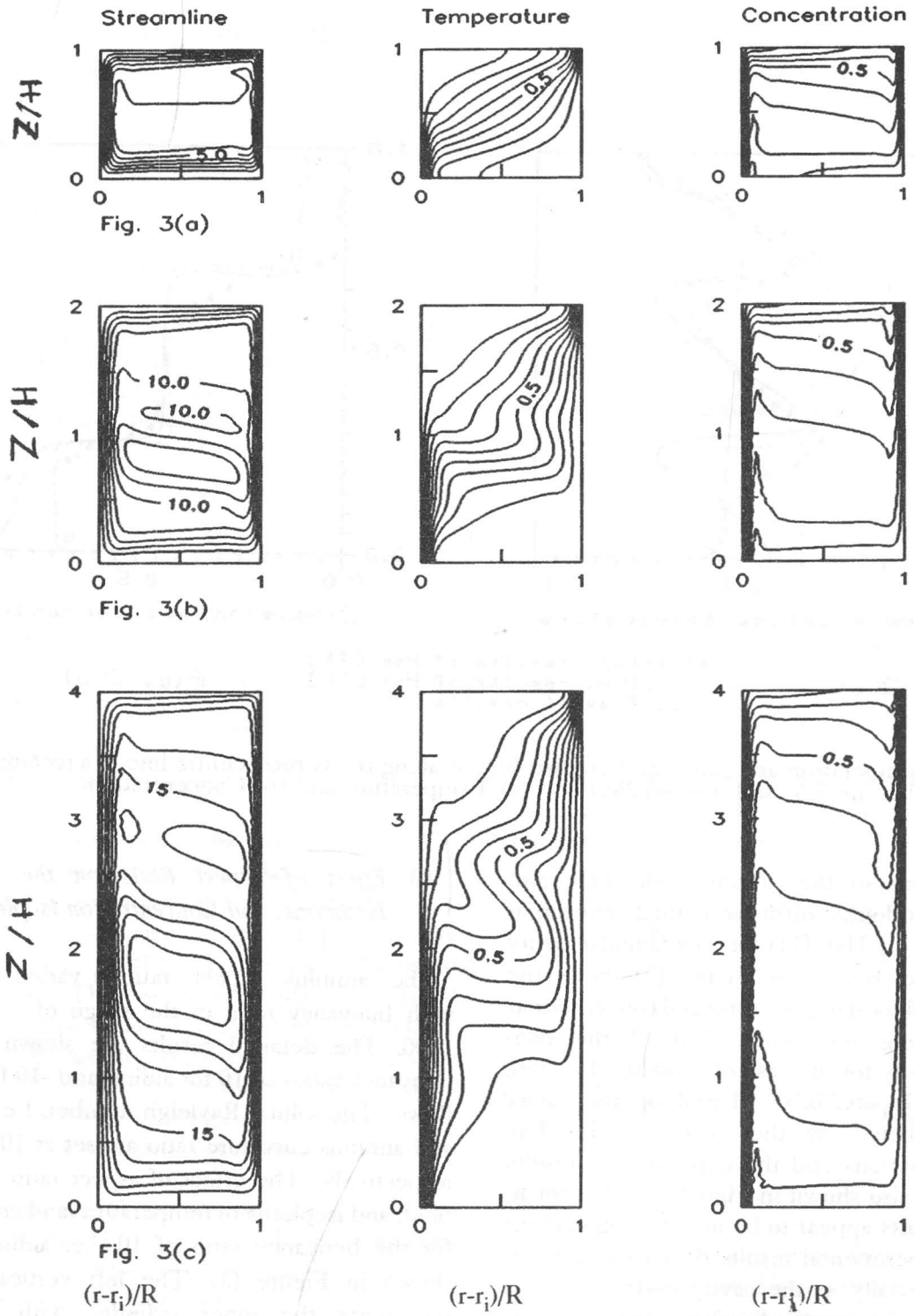

Figure 3. Effect of aspect ratio on streamlines, isotherms and iso-concentration contours for aiding flow; $Ra_m=10^5$, Le=10, n=10 and K=2; (a) Ar=1 , (b) Ar=2 and (c) Ar=4 .

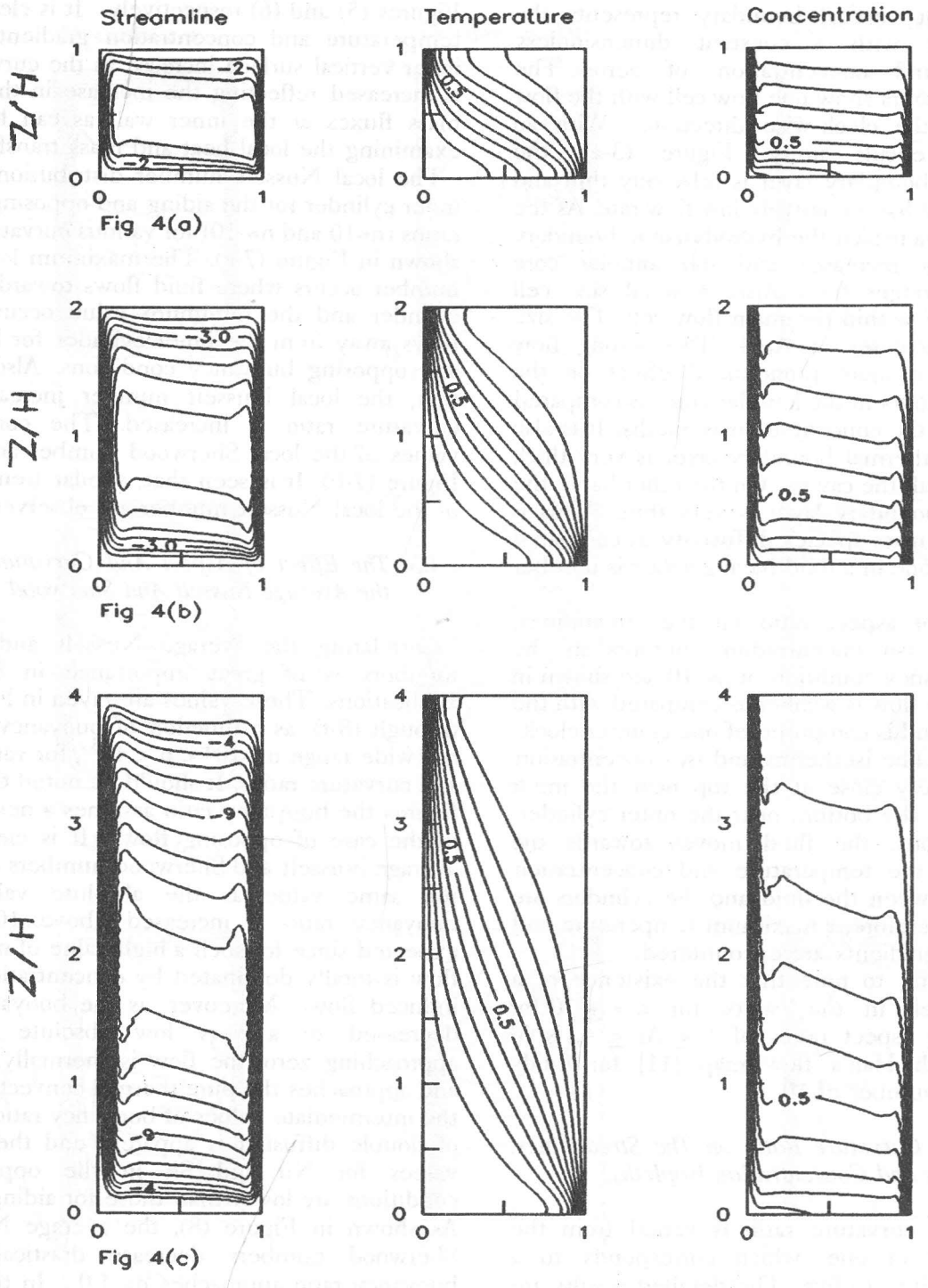

Figure 4. Effect of aspect ratio on streamlines, isotherms and iso-concentration contours for opposing flow; $Ra_m=10^5$, Le=10, n=-10 and K=2; (a) Ar=1 , (b) Ar=2 and (c) Ar=4

while the right vertical boundary represents the outer cylinder with a constant dimensionless temperature and concentration of zero. The streamline contours show one flow cell with the flow circulating in the clock-wise direction. With an aspect ratio equals unity, Figure (3-a), the hydrodynamic boundary layer is relatively thin and the annular core has a relatively low flow rate. As the aspect ratio is increased the hydrodynamic boundary layer thickness increases and the annular core develops a stronger flow. Also, a small size cell appears at Ar=2 within the main flow cell. The size of this cell increases at Ar=4. This strong flow appears to have more pronounced effect on the isothermal contours in the annular core, as compared to its effect on the concentration isopleths. It is also seen that, the thermal boundary layer is very thick and occupying all the cavity. On the other hand, the mass species boundary layer is very thin. This is due to the low mass species diffusivity as compared to the thermal one in a fluid having a Lewis number of 10.

The effect of aspect ratio on the streamlines, isotherms and iso-concentration contours in the opposing buoyancy condition of n=-10 are shown in Figure (4). The flow is weaker as compared with the previous one, and is composed of one counter clock-wise flow cell. The isotherms and iso-concentration contours are very close at the top near the inner cylinder and at the bottom near the outer cylinder. In these regions, the fluid moves towards the cylinder and the temperature and concentration differences between the fluid and the cylinders are maximum. Therefore, a maximum temperature and concentration gradients are encountered.

It is interesting to note that the existence of a single flow cell in the cavity for $n = \pm 10$ for cavities having aspect ratios of $1 \leq Ar \leq 4$, is in agreement with Han's flow map [11] for fluids having Lewis number of 10.

4.2. *Effect of Curvature Ratio on The Streamlines, Isotherms and Concentration Isopleths.*

The annulus curvature ratio is varied from the extreme value of one, which corresponds to a rectangular cavity, to five. The detailed results are shown herein for the middle aspect ratio of two while the other parameters are maintained constant at the same values given before. The effect of the annulus curvature ratio on the isopleth contours for the stream function, and dimensionless temperature and concentration for both aiding and opposing buoyancy ratios of n=10 and n=-10 are shown in Figures (5) and (6) respectively. It is clear that, the temperature and concentration gradients near the inner vertical surface increase as the curvature ratio is increased reflecting the increase in the heat and mass fluxes at the inner wall as can be seen by examining the local heat and mass transfer rates.

The local Nusselt number distribution along the inner cylinder for the aiding and opposing buoyancy ratios (n=10 and n=-10) for various curvature ratios is shown in Figure (7-a). The maximum local Nusselt number occurs where fluid flows towards the inner cylinder and the minimum value occurs where it flows away from the inner cylinder for both aiding and opposing buoyancy conditions. Also it is seen that, the local Nusselt number increases as the curvature ratio is increased. The corresponding values of the local Sherwood number are shown in Figure (7-b). It is seen that, similar trends to those of the local Nusselt number are observed.

4.3. *The Effect of Aspect And Curvature Ratios on the Average Nusselt And Sherwood Numbers.*

Correlating the average Nusselt and Sherwood numbers is of great importance in engineering applications. These values are given in Figures (8-a) through (8-f), as a function of buoyancy ratio, over the wide range of $-10^3 \leq n \leq 10^3$, for various aspect and curvature ratios. It should be noted that in these figures the buoyancy ratio assumes a negative value in the case of opposing flow. It is clear that the average Nusselt and Sherwood numbers converge to the same value as the absolute value of the buoyancy ratio is increased above 100. This is expected since for such a high value of n the overall flow is totally dominated by concentration gradient induced flow. Moreover, as the buoyancy ratio is decreased to a very low absolute value, i.e. approaching zero, the flow is thermally dominated and approaches the pure thermal convection case. In the intermediate values of buoyancy ratio, the effect of double diffusion is apparent and the calculated values for Nu and Sh in the opposing flow conditions are lower than those for aiding flow case. As shown in Figure (8), the average Nusselt and Sherwood numbers decrease drastically as the buoyancy ratio approaches n=-1.0 . In this case the two driving forces are equal but in opposite directions and the flow accordingly is slowed down significantly. Under such condition,the flow is driven by thermal buoyancy, since the thermal diffusivity is higher than the mass diffusivity (Le=10.).

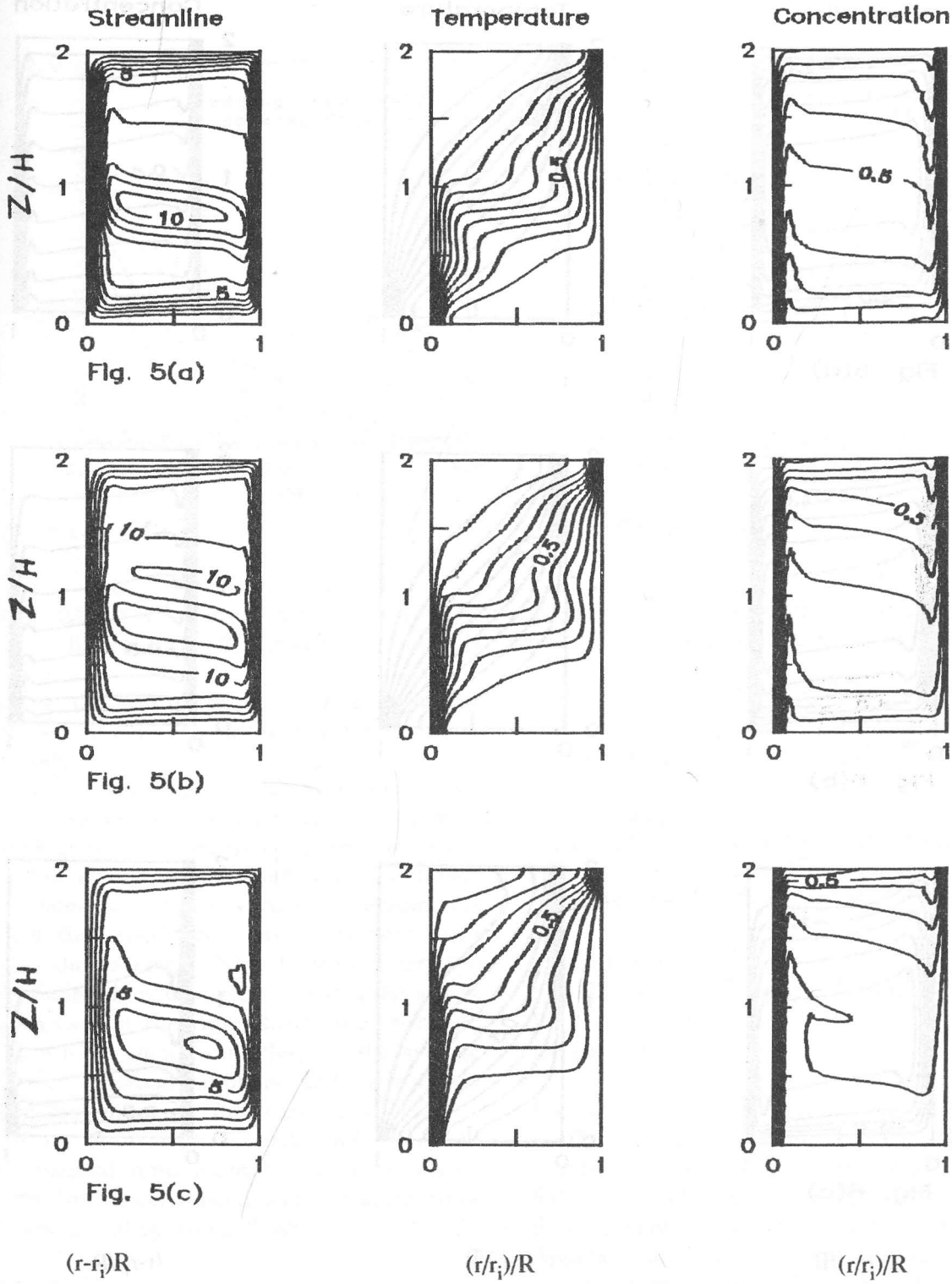

Figure 5. Effect of curvature ratio on streamlines, isotherms and iso-concentration contours for aiding flow; $Ra_m=10^5$, Le=10, n=10 and Ar=2; (a) K=1 , (b) K=2 and (c) K=5 .

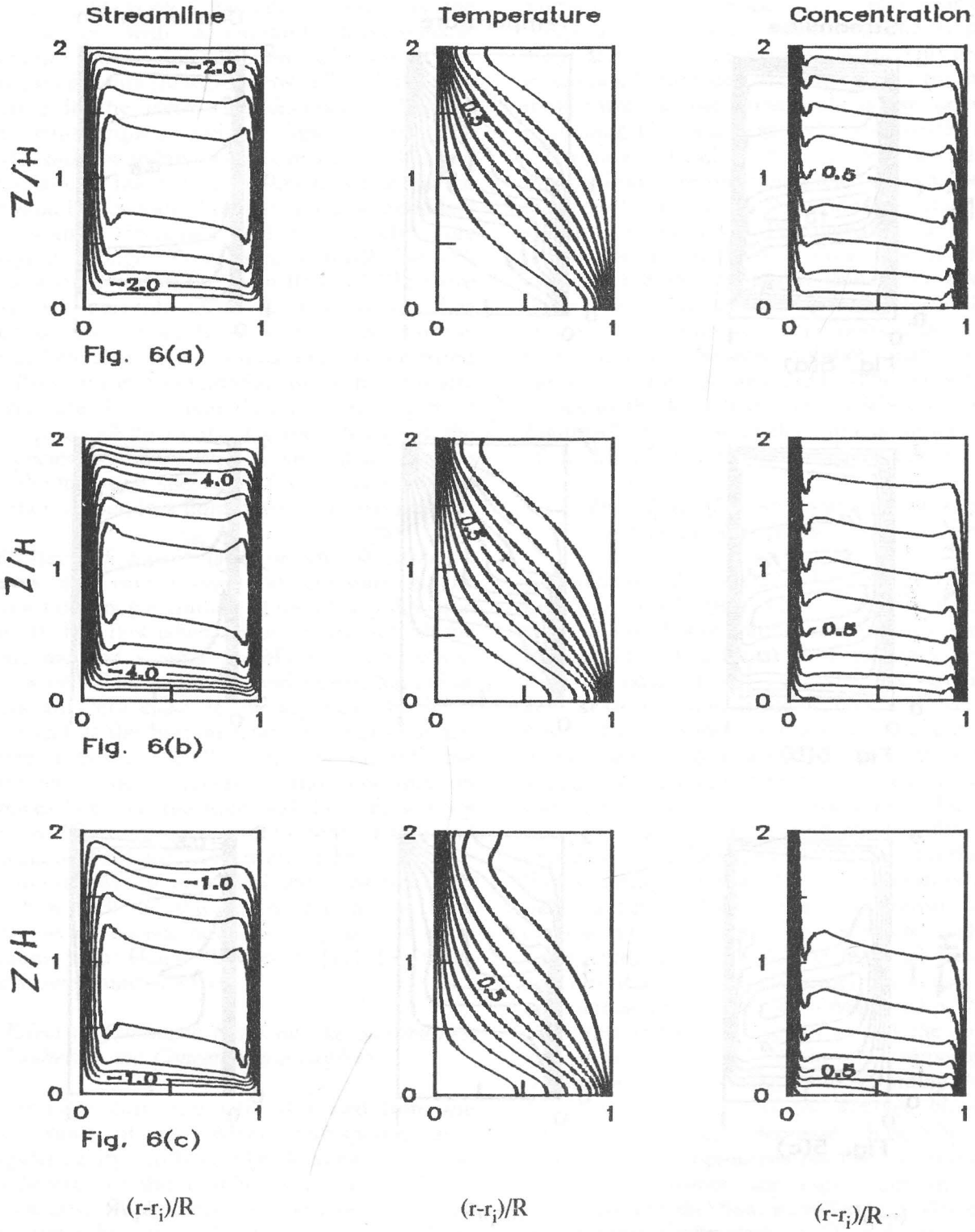

Figure 6. Effect of curvature ratio on streamlines, isotherms and iso-concentration contours for opposing flow; $Ra_m=10^5$, Le=10, n=-10 and Ar=2, (a) K=1 , (b) K=2 and (c) K=5.

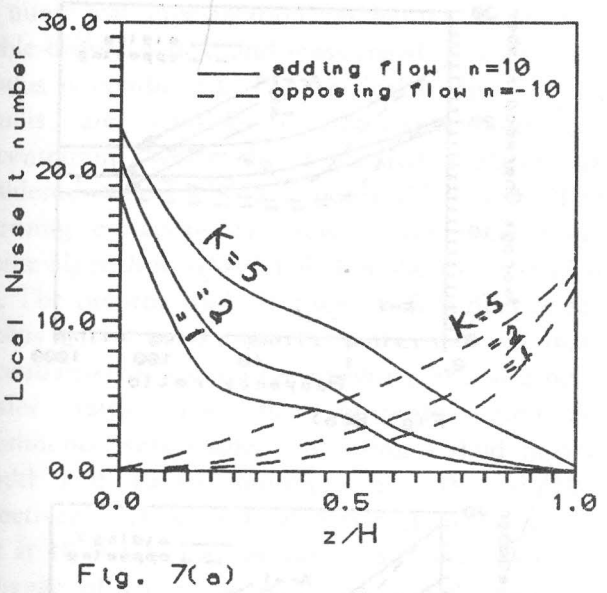

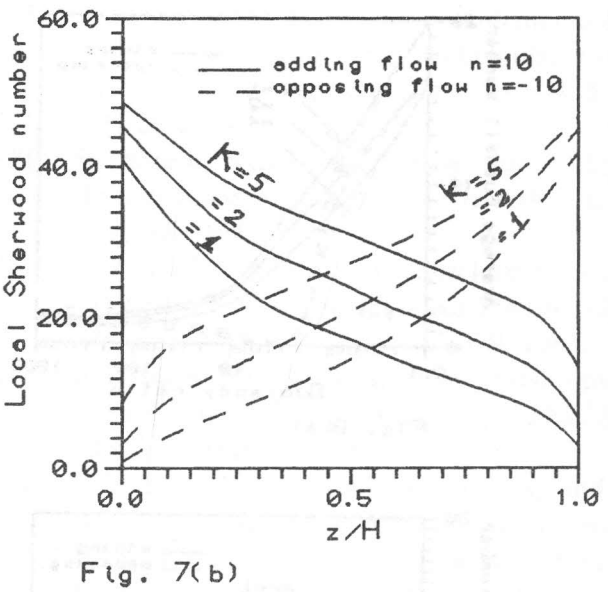

Figure 7. Effect of curvature ratio on local Nusselt and Sherwood number distributions along the inner cylinder; $Ra_m=10^5$, Le=10. and Ar=2; (a) Nusselt number and (b) Sherwood number

If Le=1.0, this will result in complete stagnation and the heat and mass transfer will be by molecular diffusion only.

The figure also shows that the average Nusselt and Sherwood numbers in the thermally driven flow region are higher than those for concentration driven flows. This is due to the high value of Lewis number. Under the conditions examined herein, it is shown that the aspect ratio has a relatively small effect on the average Nusselt and Sherwood numbers; their values increase slightly as the aspect ratio increases. On the other hand, the curvature ratio have a more significant effect on the average Nusselt and Sherwood numbers, and their values increase as the curvature ratio is increased.

The values of average Nusselt and Sherwood numbers obtained in the present work are correlated in terms of buoyancy, aspect, and curvature ratios for both aiding and opposing flows:

(i) aiding flow:

$$Nu=5.139 \times n^{-0.06592} \times Ar^{-0.12} \times K^{0.388} \quad \text{for } n>5.0$$

$$Nu=10.22 \times n^{-0.2378} \times Ar^{-0.161} \times k^{0.344} \quad \text{for } n<2.0$$

$$Sh=19.254 \times n^{-0.02096} \times Ar^{-0.185} \times K^{0.364} \quad \text{for } n>5.0$$

$$Sh=20.4503 x n^{-0.1119} x Ar^{-.18} x K^{0.4385} \quad \text{for } n<2.0 \quad (18)$$

(ii) opposing flow:

$$Nu=2.395x|n|^{.0475} x\ Ar^{-0.0946} x k^{0.455} \quad \text{for } |n|>5.0$$

$$Nu=9.392x|n|^{-0.2754} x Ar^{-.1778} x K^{0.3354} \quad \text{for } |n|<2.0$$

$$Sh=14.154x|n|^{0.0342} x Ar^{-0.19113} x K^{0.3324} \quad \text{for } |n|>5.0$$

$$Sh=17.238x|n|^{-0.19461} x Ar^{-0.18454} x K^{0.43778}$$

$$\text{for } |n|<2.0 \quad (19)$$

For all the above correlations, the correlation coefficients are 95% or better. However, the number of cases studied in the range of $2.0<|n|<5.0$ was not large enough to support the development of accurate correlations for this range. Approximate values for the average Nusselt and Sherwood numbers in the range of $2.0<|n|<5.0$ can be obtained by extending the applicability of the above correlations to $|n| = 3.5$. In this case the maximum error was found to be in the order of 15%.

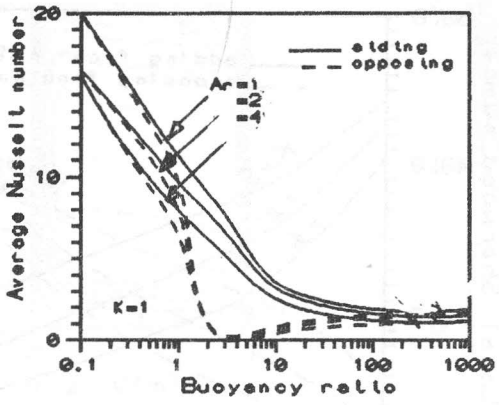

Fig. 8(a)

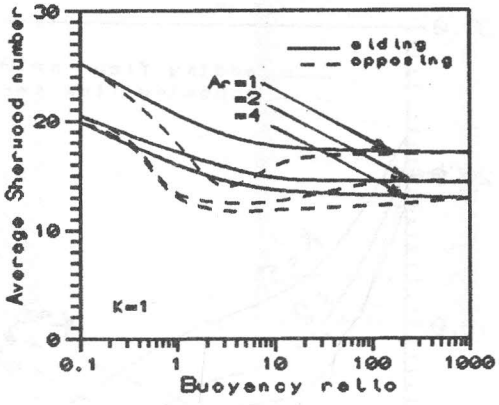

Fig. 8(b)

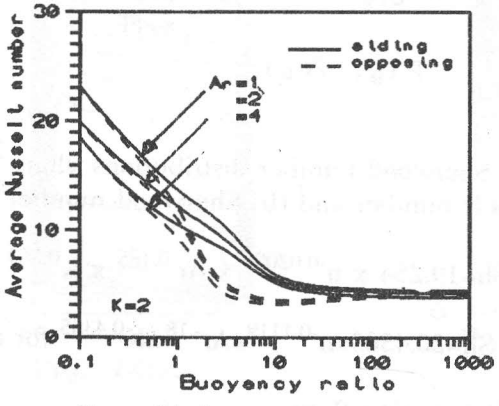

Fig. 8(c)

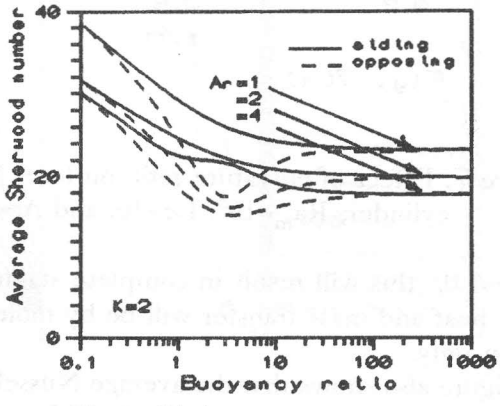

Fig. 8(d)

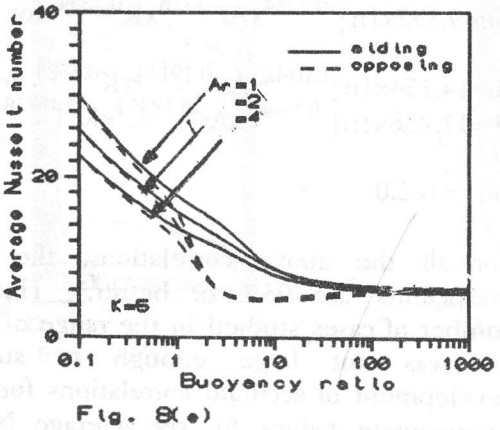

Fig. 8(e)

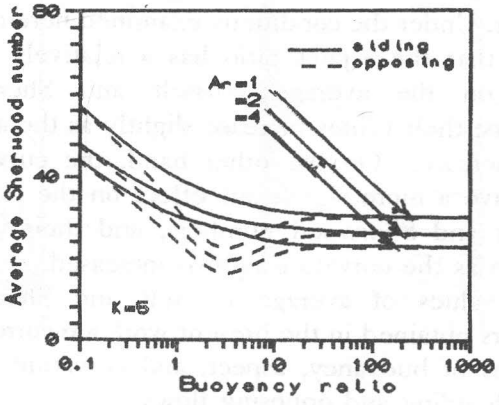

Fig. 8(f)

Figure 8. The effect of buoyancy ratio, aspect ratio and curvature ratio on both average Nusselt and Sherwood numbers.

5. CONCLUDING REMARKS

A numerical investigation on natural convection double-diffusive heat and mass transfer in a vertical annulus is conducted. The vertical surfaces of the annulus are considered isothermal and iso-concentration, while the horizontal surfaces are considered adiabatic and impermeable plates. The governing equations are solved using the finite volume algorithm SIMPLER described by Patankar [18]. The present study focuses on the effect of the annulus geometry on the flow, thermal and mass concentration fields and the resulting heat and mass transfer rates. For this purpose, numerical experiments were carried out using a fluid having Prandtl and Lewis numbers of 8.0 and 10.0 respectively. The solutal Rayleigh number was kept at 10^5 while the buoyancy ratio was varied in the range of $10^3 \geq |n|$ covering a wide range of flows driven by the separate and combined effects of both thermal and concentration gradients. The study was carried out by varying the annulus aspect and curvature ratios in the range of $1 \leq Ar \leq 4$ and $1 \leq K \leq 5$.

Within the range of the present parameters, the flow structure is mainly a uni-cell structure whose flow direction is dependent on the more dominated driving force. The uni-cell flow structure was maintained even in the range of buoyancy numbers where both driving forces are important. With the uni-cell flow structure, the local Nusselt and Sherwood numbers were found to increase or decrease systematically along the vertical walls depending on the circulation direction. The maximum values of the local Nusselt and Sherwood numbers were encountered where the circulating flow is moving towards the wall.

The results also showed that the curvature ratio has a more pronounced effect on the average Nusselt and Sherwood numbers as compared to the aspect ratio. The average Nusselt and Sherwood numbers were correlated in terms of buoyancy, aspect and curvature ratios in the range of the examined conditions.

6. REFERENCES

[1] C.Y. Hu, M.M. EL-Wakil, Simultaneous heat and mass transfer in a rectangular cavity, *Proc. 5th Int. Heat Transfer Conf.* vol. 5, pp. 24-28 1974.

[2] S. Ostrach, Natural convection with combined driving forces, *Physico Chem Hydrdyn*, 1, pp. 233-247, 1980.

[3] S. Ostrach, Natural convection heat transfer in cavities and cells, 7th *Int. Heat Transfer Conf.*, Munich, 1982, vol. 1, pp. 365-379, 1983.

[4] S. Ostrach, Fluid mechanics in crystal growth-the 1982 freeman scholar lecture, *J. Fluid Eng.* 105, 5-20 March, 1983.

[5] T.S. Lee, P.G. Parikh, A. Acrivos, and D. Bershader, Natural convection in a vertical channel with opposing buoyancy forces, *Int. J. Heat Mass Transfer*, 25, 499-511, 1982.

[6] S. Kimura, and A. Bejan, The boundary layer natural convection regime in a rectangular cavity with uniform heat flux from the side, *ASME J. Heat Transfer*, 106, 98-103, 1984.

[7] O.V. Trevisan, and A. Bejan, Combined heat and mass transfer by natural convection in a vertical enclosure, *ASME J. Heat Transfer*, 109, 104-112, 1987.

[8] P. Ranganathan, and R. Viskanta, Natural convection in a square cavity due to combined driving forces, *J. Numerical Heat Transfer*, 14, 35-59, 1986.

[9] C. Beghein, F. Haghighat and F. Allard, Numerical study of double-diffusive natural convection in a square cavity, *Int. J. Heat Mass Transfer*, 35, 833-846, 1992.

[10] H. Han and T. H. Kuehn, Double diffusive natural convection in a vertical rectangular enclosure - I experimental study, *Int. J. Heat Mass Transfer*, 34, 449-459, 1991.

[11] H. Han and T.H. Kuehn, Double diffusive natural convection in a vertical rectangular enclosure - II numerical study, *Int. J. Heat Mass Transfer*, 34, 461-471, 1991.

[12] J.M. Hyun and J.W. Lee, Double diffusive convection in a rectangle with cooperating horizontal gradients of temperature and concentration, *Int. J. Heat Mass Transfer*, 33, 1605-1617, 1990.

[13] J.W. Lee and J.M. Hyun, Double diffusive convection in a rectangle with opposing horizontal temperature and concentration gradients, *Int. J. Heat Mass Transfer*, 33, 1619-1632, 1990.

[14] J.W. Lee and J.M. Hyun, Double diffusive convection in a cavity under a vertical solutal gradient and a horizontal temperature gradient, Int. *J. Heat Mass Transfer*, 34, 2423-2427 1991.

[15] P.W. Shipp, Numerical simulation of double diffusive natural convection within a closed annulus, M.Eng. Thesis University of McMaster, Hamilton, Ontario, Canada, 1991.

[16] P.W. Shipp, M. Shoukri and M. B. Carver, Double-diffusive natural convection in a closed annulus, Submitted to *Numerical Heat Transfer*, 1992.

[17] P.W. Shipp, M. Shoukri and M.B. Carver, The effect of thermal Rayleigh and Lewis numbers on double-diffusive natural convection in a closed annulus, Submitted to *Numerical Heat Transfer*, 1992.

[18] S.V. Patankar, Numerical heat transfer and fluid flow, Hemisphere Washington, DC. 1980.

[19] G. De Vahl Davis and R.W. Thomas, Natural convection in annular and rectangular cavities-A numerical studies, Proceeding Forth *Int. Heat Transfer Conf.*, Paris, vol.4, NC2.4, Elsevier, Amsterdam, 1970.

[20] G. De Vahl Davis, Natural convection of air in a square cavity: a benchmark numerical solution, *Int. J. Numer. Meth. Fluids*, vol.3, 249-264, 1983.

[21] S.M. ElSherbiny and M.A. Teamah, Natural convection in annular vertical cavities, Fourth *Int. Conf. of Fluid Mechanics, Alex.*, Egypt April 28-30, 1992.